MTPA Trajectory Tracking Control with On-line MRAS Parameter Identification for an IPMSM

Ningzhi Jin[1] · Guangyi Li[1] · Kai Zhou[1] · Jinfeng Liu[1] · Herbert Ho-Ching Iu[2]

Abstract

The maximum torque per ampere (MTPA) control is capable of obtaining its maximal ratio of torque to current in a control system of interior permanent magnet synchronous motor (IPMSM). However, when its electrical parameters change with the actual operating conditions, the resulting MTPA trajectory will deflect from the optimal one. To solve this problem, a modified model reference adaptive system (MRAS) method is investigated for the parameter identification of the rotor flux linkage and the stator q-axis inductance, after a tradeoff between the MTPA trajectory derivation degree with parameter change and the rank-deficiency problem in the identification model. In this method, a full-rank estimator and its gain matrix are designed according to the Popov Hyper Stability Theorem. And the current operating point is updated using the identified parameters in order for the real-time tracking of MTPA trajectory. Simulation and experimental results verify that the proposed method enhances remarkably the MTPA tracking control effect and the system's torque-current characteristics for an IPMSM.

1 Introduction

Due to its firmer configuration, lower torque pulsation, wider speed range and higher power density, an interior permanent magnet synchronous motor (IPMSM) is extensively used in numerous traditional and emerging industrial fields, such as numerical control machine tools, wind power generation and electrical vehicles (EV), and especially becomes the first choice of EV tractions. For an IPMSM control system, to design an appropriate distribution theme for its stator current and make rational use of the resulting reluctance torque is greatly beneficial to improving the torque/speed output characteristics and the system's operation efficiency [1, 2].

The maximum efficiency control is one of the most important design criteria in many industrial application fields. For example, the operation efficiency is a critical performance indicator in a motor drive and control system of EV powered by batteries. In an IPMSM's operation area below the flux-weakening speed, its stator copper loss plays a major role compared with ignorantly slight iron loss and rotor copper loss. Thus, the maximum torque per ampere (MTPA) control can be considered as a kind of the maximum efficiency control, which is able to output the maximal torque with a certain stator current or to generate a certain torque with the minimal stator current and copper loss, aiming at increasing the system's operation efficiency [3, 4].

An accurate mathematical model should be established with accurate pre-known parameters in order to obtain an optimal current vector complying with the MTPA definition. Nevertheless, an IPMSM's electrical parameters, including the rotor flux linkage, the stator inductance and the stator resistance, may be time-varying with the actual inconstant operating speed and torque due to temperature rise, magnetic saturation, armature reaction, etc. And in general, the constant parameters were used in the traditional control methods, and an approximate and average MTPA trajectory was

✉ Ningzhi Jin
   sharon0716@126.com

1   Engineering Research Center of Automotive Electronics
    Drive Control and System Integration, Ministry
    of Education, Harbin University of Science and Technology,
    Harbin 150080, China

2   School of Electric, Electronic and Computer Engineering,
    University of Western Australia, Perth, WA 6009, Australia

designed in the total working range, probably significantly inconsistent with the optimal one as a result of parameter variance.

The iterative method could not deduce an accurate function model and has not taken any effect of parameter change into consideration [5]. In the look-up table (LUT) method, the calculation complexity was simplified and the parameters were partially considered, but a huge amount of memory spaces were taken up and a heavy burden was placed on the off-line test [6]. The MTPA trajectory could be automatically approached under the condition of parameter variance with the auto-tracking method, which caused low convergence speed and low torque control accuracy [7]. The signal injection method was able to modify the present operating point according to the torque ripple generated by the injected signal so as for the real-time tracking of MTPA trajectory [8, 9]. However, the injected high-frequency current may result in additional torque ripple and power loss.

Consequently, the parameter identification method should be applied to enhance the system's MTPA control properties. Nowadays, there are several practical and effective methods of parameter identification, including recursive least square method (RLS), extended Kalman filter method (EKF), model reference adaptive system method (MRAS) and neutral network method (NN).

In the RLS method, it is a must to store the necessary data from the former step during the current step of recursive calculation, which inevitably brings about data saturation [10–12]. In [10], a RLS method with a variable forgetting factor was used to estimate an IPMSM's dq-axis inductances and resistance, which improved the identification accuracy and rate of convergence. A novel quasi-steady-state multi-parameter identification method for an SPMSM was proposed in [11], that is, the three parameters (flux linkage, inductance and resistance) were estimated in two steps using constant-current acceleration process and current injection. In [12], the influence of parameter variance on the MTPA control characteristics was analyzed, and a fast estimator was designed to estimate the d-q inductances while a slow one identified the rotor flux linkage and the stator resistance.

For a sensorless control system, its rotor position and speed can be well identified with the EKF method. However, the method has several obstacles to the identification of an IPMSM's parameter. For instance, the flux linkage is identified in a 4th-order model causing a huge amount of real-time computing, and even in the low speed or light load, the smaller inputs or larger noises result in larger estimated errors [13]. Two estimators were separately designed with the MRAS method and the EKF method in [13], and it was shown that the latter method did not take on better estimation effect although its algorithm was more complex.

The design intentions of MRAS is that the adjustable model's parameters are adjusted and identified with the predesigned adaptive laws, for the purpose of their progressive convergence to the real parameters in the reference model [14–17]. An estimator based on the Lyapunov Stability Theorem was designed and compared with the one using the Popov Hyper Stability Theorem in [14], and it was pointed out that the latter method had better tracking responses of parameter change with a integral item besides a proportional one. The three SPMSM electrical parameters were identified simultaneously in [15], but a rank-deficiency problem in the system model was ignored, which may give rise to multiple convergence results. In [16], firstly, the inductance was estimated in the q-axis current equation. Then, the resistance and flux linkage were identified with d-axis current injection. This method could overcome the rank-deficiency problem in the multi-parameter identification and ensure the uniqueness of estimated results.

The neutral network (NN) method can obtain excellent convergence characteristics, whereas the practical and extensive use was greatly confined due to its very complex algorithm [18, 19]. In [18], the three parameters of an SPMSM were estimated with a combination of on-line and off-line methods, which was unable to meet the high demand of real-time performance. A two-step method with injected current was presented for an SPMSM in [19]. In this method, considering the inverter's nonlinearity, an identification model without voltage error was built up so as to enhance the identification accuracy.

Nevertheless, an IPMSM's 3 parameters should be estimated and used for the MTPA trajectory tracking. At the same time, the estimator's rank is 2, elaborated later in Sects. 2 and 3. As a result, the 2nd-order rank-deficiency model cannot guarantee that all the 3 parameters converge simultaneously with a certain degree of precision. In summary, the current solutions to the rank-deficiency problem now focus mainly on as follows:

1. Only 1 or 2 parameters were estimated on-line, while the rest ones were assumed to be constant or estimated off-line without consideration of the impact of parameter change on the MPTA control qualities [17, 18].
2. At least 2 parameters were identified simultaneously, but the rank-deficiency problem in the model was neglected. Hence, there are inadequate evidences in theory to support the uniqueness of convergent values [13–15].
3. A step-by-step method was adopted in which some parameters were identified on-line at the first step, and then the other ones were obtained with current injection in order to increase the system's operation states and the model's rank. However, the injected current had a bad influence on the torque control and identification accuracy, and the multi-step process worsened the system's dynamic responses [10–12, 16, 19].

In conclusion, a modified MRAS-based method of parameter identification is introduced for the MTPA tracking control of an IPMSM. Initially, the variation tendency of MTPA trajectories is assessed under the condition of changeable parameters. After that, a full-rank estimator and its gain matrix on the flux linkage and the q-axis inductance are designed in accordance with the Popov Hyper Stability Theorem. Finally, the current operating point is recalculated and refreshed with the identified parameters in order for the on-line tracking of MTPA trajectory.

2 IPMSM Model and MTPA Control

The dq-axis equation of an IPMSM's stator voltages can be described as

$$\begin{cases} u_d = R_s i_d + L_d \dfrac{di_d}{dt} - L_q \omega_e i_q \\ u_q = R_s i_q + L_q \dfrac{di_q}{dt} + L_d \omega_e i_d + \omega_e \psi_f \end{cases} \tag{1}$$

where i_d and i_q are the dq-axis currents, u_d and u_q are the dq-axis voltages, Ψ_f is the rotor permanent magnet flux linkage, R_s is the phase resistance, L_d and L_q are the dq-axis inductances, and ω_e is the rotor electrical angular speed.

The corresponding electromagnetic torque is

$$T_e = 1.5p(\psi_f i_q + (L_d - L_q)i_d i_q) \tag{2}$$

where p is the number of pole pairs.

Using the toque angle β between q-axis and the stator current i_s, i_d and i_q can be written as

$$\begin{cases} i_d = -i_s \sin \beta \\ i_q = i_s \cos \beta \end{cases} \tag{3}$$

If a stator current control method is aiming at generating a certain torque with the least current amplitude or outputting the highest torque with a given current value, it is named as the maximum torque per ampere control (MTPA) [3]. For the purpose of a maximal ratio of T_e to i_s, the torque angle β should be set as

$$\sin \beta = \frac{\psi_f - \sqrt{\psi_f^2 + 8(L_d - L_q)^2 i_s^2}}{4(L_d - L_q)i_s} \tag{4}$$

Obviously, the expected values of the dq-axis currents can be calculated on-line according to Eqs. (3)–(4) in order to track the MTPA trajectory real-timely. However, in the actual operation of an IPMSM, its key electrical parameters, the rotor flux linkage and the dq-axis inductances included, must be variable with temperature rise, magnetic saturation, armature reaction, etc. As a result, the actual MTPA trajectory must be inconsistent with its optimal one due to the parameter change.

3 Influence of Parameter Variance on MTPA Trajectories

The stator resistance R_s becomes higher due to its temperature rise and appears to be an approximate linear-function of the temperature. Also, the rotor flux linkage Ψ_f will decrease if the temperature increases. Accordingly, the change in the flux density and magnetic permeability will influence on the stator inductance.

More importantly, the phenomenon of magnetic saturation will have effect on the stator inductance, i.e., the stator and rotor core exhibits a nonlinear current-flux feature and thus the inductance variance. Figure 1 reveals the variation tendency of dq-axis inductances with the stator current.

When i_d is tiny, the d-axis magnetic field Ψ_d is saturated to a certain extent, so L_d is almost unchangeable; otherwise, especially in the flux-weakening working area, Ψ_d will be greatly weakened, which reduces L_d slowly with the negative increase of i_d. On the other hand, the magnetic saturation influences on L_q more significantly. When i_q is smaller and the q-axis magnetic field Ψ_q is linear with respect to i_q, L_q approximates a constant; or in the saturated zone of Ψ_q, L_q goes down quickly with the positive increase of i_q. In a word, for the whole operation range, L_d varies within a very small range and with a lower speed.

Additionally, Ψ_d affects its quadrature magnetic field Ψ_q, or vice versa, called armature reaction or cross coupling. As expressed in the stator voltages Eq. (1), there is a coupling item $-L_q \omega_e i_q$ in the d-axis equation and a coupling item $+L_d \omega_e i_d$ in the q-axis equation, too.

As Fig. 2 shows, when L_d, L_q and Ψ_f change within $\pm 10\%$ of their respective average values, the actual current working points deflect from the optimal MTPA trajectory under the condition of parameter change.

It is obvious that the variance of L_q or Ψ_f give rise to a significant derivation of the MTPA trajectory and operating
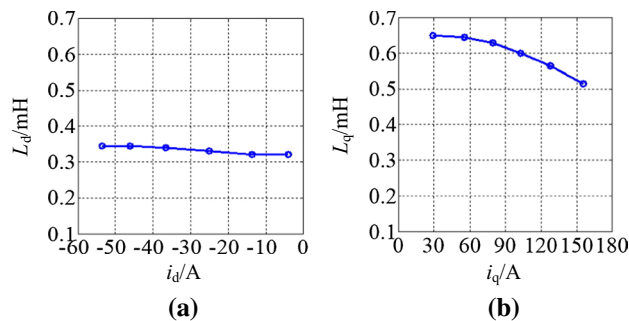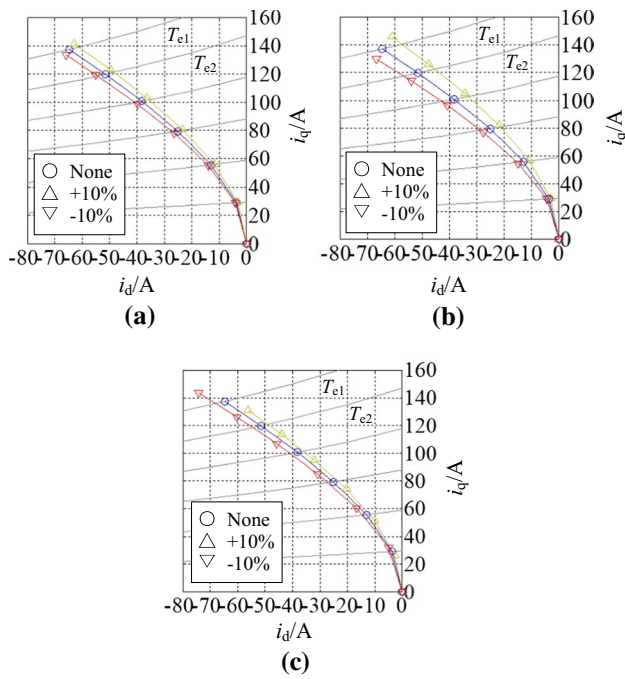

Fig. 1 Inductance variances

Fig. 2 MTPA trajectory derivations with parameter variances. **a** L_d. **b** L_q. **c** Ψ_f
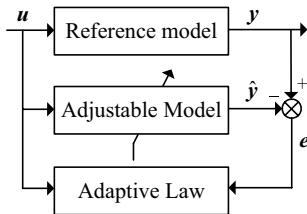

Fig. 3 Model reference adaptive system

point, while that of L_d brings about only a negligible trajectory derivation.

As mentioned above, weighing between the rank-deficiency phenomenon in the estimator's model and the MTPA control performances, a new method of parameter identification is presented and designed for the MTPA tracking control of an IPMSM, in which L_q and Ψ_f are identified on-line with an assumption of a constant L_d.

4 Model Reference Adaptive System of IPMSM

4.1 Structure of Model Reference Adaptive System

The structure diagram of a model reference adaptive system (MRAS) is depicted in Fig. 3. In this system, the predesigned adaptive laws force the output error e (between

the reference model's output y and the adjustable model's output $\hat{y}$) to converge to zero, with which the parameters are adjusted and identified. That is to say that the adjustable model's parameters to be identified will be approaching asymptotically the reference model's real parameters.

Mapping an IPMSM into the system as Fig. 3 depicts, the system input is $\boldsymbol{u} = \begin{bmatrix} u_d & u_q \end{bmatrix}^T$, the reference model's output is $\boldsymbol{y} = \boldsymbol{i} = \begin{bmatrix} i_d & i_q \end{bmatrix}^T$, the adjustable model's output is $\hat{\boldsymbol{y}} = \hat{\boldsymbol{i}} = \begin{bmatrix} \hat{i}_d & \hat{i}_q \end{bmatrix}^T$, and the output error is $\boldsymbol{e} = \boldsymbol{i} - \hat{\boldsymbol{i}}$.

4.2 IPMSM's Reference Model

For an IPMSM control system, the state space equation of dq-axis currents is derived from Eq. (1) as

$$
\begin{bmatrix} \frac{di_d}{dt} \\ \frac{di_q}{dt} \end{bmatrix} = \begin{bmatrix} -\frac{R_s}{L_d} & \frac{L_q}{L_d}\omega_e \\ -\frac{L_d}{L_q}\omega_e & -\frac{R_s}{L_q} \end{bmatrix} \begin{bmatrix} i_d \\ i_q \end{bmatrix} + \begin{bmatrix} \frac{1}{L_d} & 0 \\ 0 & \frac{1}{L_q} \end{bmatrix} \begin{bmatrix} u_d \\ u_q \end{bmatrix} + \begin{bmatrix} 0 \\ -\frac{\psi_f}{L_q}\omega_e \end{bmatrix}
$$
(5)

Regarding Eq. (5) as an IPMSM's reference model follows that

$$\dot{\boldsymbol{i}} = A\boldsymbol{i} + B\boldsymbol{u} + C \tag{6}$$

where,

$$
A = \begin{bmatrix} -\frac{R_s}{L_d} & \frac{L_q}{L_d}\omega_e \\ -\frac{L_d}{L_q}\omega_e & -\frac{R_s}{L_q} \end{bmatrix}, \quad B = \begin{bmatrix} \frac{1}{L_d} & 0 \\ 0 & \frac{1}{L_q} \end{bmatrix}, \quad C = \begin{bmatrix} 0 \\ -\frac{\psi_f}{L_q}\omega_e \end{bmatrix}
$$

4.3 Parameter Adjustable Model

Assuming that the rotor speed ω_e is invariable during the process of parameter estimation, from the reference model Eq. (6), the adjustable model is established as

$$\dot{\hat{\boldsymbol{i}}} = \hat{A}\hat{\boldsymbol{i}} + \hat{B}\boldsymbol{u} + \hat{C} - G\boldsymbol{e} \tag{7}$$

where,

$$
\hat{A} = \begin{bmatrix} -\frac{R_s}{L_d} & \frac{\hat{L}_q}{L_d}\omega_e \\ -\frac{L_d}{\hat{L}_q}\omega_e & -\frac{R_s}{\hat{L}_q} \end{bmatrix}, \quad \hat{B} = \begin{bmatrix} \frac{1}{L_d} & 0 \\ 0 & \frac{1}{\hat{L}_q} \end{bmatrix}
$$

$$
\hat{C} = \begin{bmatrix} 0 \\ -\frac{\hat{\psi}_f}{\hat{L}_q}\omega_e \end{bmatrix}, \quad G = \begin{bmatrix} -g_{11} & -g_{12} \\ g_{21} & -g_{22} \end{bmatrix}
$$

To select an appropriate gain matrix G, the parameter estimator can obtain desirable convergence properties and achieve anticipant asymptotic stability.

The system's error equation can be deduced by Eq. (6) minus Eq. (7)

$$\dot{\boldsymbol{e}} = (A + G)\boldsymbol{e} + \Delta A\hat{\boldsymbol{i}} + \Delta B\boldsymbol{u} + \Delta C \tag{8}$$

where $\Delta A = A - \hat{A}$, $\Delta B = B - \hat{B}$, and $\Delta C = C - \hat{C}$.

5 Design of MRAS Parameter Estimator

This paper designs a MRAS parameter estimator in terms of the Popov Hyper Stability Theorem [20].

5.1 Equalization of Nonlinear Feedback System

With a definition of $w = -(\Delta A \hat{i} + \Delta B u + \Delta C)$, the parameter identification model Eq. (8) can be reconstructed as

$$\dot{e} = (A + G)e - w \tag{9}$$

From the above equation, an equivalent nonlinear time-varying feedback system can be illustrated as in Fig. 4, where $\varphi(e)$ stands for the parameters' adaptive law.

5.2 Design of Adaptive Law

The Popov Integral Inequality is

$$\eta(0, t_1) = \int_0^{t_1} e^{\mathrm{T}} w \mathrm{d}t \geq -\gamma^2 \tag{10}$$

where a constant γ is positive and limited free of $t \geq 0$.

Substituting e and w into Eq. (10), it follows two sub inequalities concerning the identified parameters L_q and Ψ_f

$$
\begin{cases}
\eta_1(0, t_1) = \int_0^{t_1} (\frac{1}{\hat{L}_q} - \frac{1}{L_q})[(u_q - R_s \hat{i}_q - \omega_e L_d \hat{i}_d)(i_q - \hat{i}_q) \\
\qquad\qquad - \frac{L_q}{L_d} \omega_e L_q \hat{i}_q (i_d - \hat{i}_d)] \mathrm{d}t \geq -\gamma_1^2 \\
\eta_2(0, t_1) = \int_0^{t_1} -(\frac{\hat{\psi}_f}{\hat{L}_q} - \frac{\psi_f}{L_q}) \omega_e (i_q - \hat{i}_q) \mathrm{d}t \geq -\gamma_2^2
\end{cases}
\tag{11}
$$

In general, the adaptive law in reference to L_q is described as

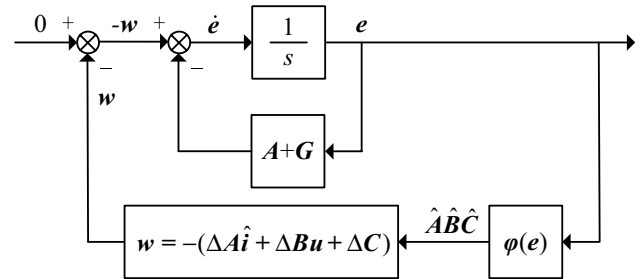$$\frac{1}{\hat{L}_q} = \frac{1}{L_q} + f_1(t) + \int_0^t f_2(\tau) \mathrm{d}\tau \tag{12}$$

Fig. 4 Nonlinear feedback system

From Eq. (11) and Eq. (12), we get

$$
\begin{cases}
\eta_{11}(0, t_1) = \int_0^{t_1} [(u_q - R_s \hat{i}_q - L_d \hat{i}_d \omega_e)(i_q - \hat{i}_q) \\
\qquad\qquad - \frac{L_q}{L_d} \omega_e L_q \hat{i}_q (i_d - \hat{i}_d)] f_1(t) \mathrm{d}t \geq -\gamma_{11}^2 \\
\eta_{12}(0, t_1) = \int_0^{t_1} [(u_q - R_s \hat{i}_q - L_d \hat{i}_d \omega_e)(i_q - \hat{i}_q) \\
\qquad\qquad - \frac{L_q}{L_d} \omega_e L_q \hat{i}_q (i_d - \hat{i}_d)] \int_0^t f_2(\tau) \mathrm{d}\tau \mathrm{d}t \geq -\gamma_{12}^2
\end{cases}
\tag{13}
$$

Hence, the adaptive law regarding L_q can be deduced

$$\frac{1}{\hat{L}_q} = \frac{1}{L_q} + \left(k_1 + \frac{1}{\tau_1 s}\right) \left[(u_q - R_s \hat{i}_q - \omega_e L_d \hat{i}_d)(i_q - \hat{i}_q) \right. $$
$$\left. - \frac{L_q}{L_d} \omega_e L_q \hat{i}_q (i_d - \hat{i}_d) \right] \tag{14}$$

where k_1 and τ_1 represent the PI coefficients of L_q's adaptive law.

Similarly, the adaptive law regarding the parameter Ψ_f can also be deduced

$$\frac{\hat{\psi}_f}{\hat{L}_q} = \frac{\psi_f}{L_q} - \left(k_2 + \frac{1}{\tau_2 s}\right) \omega_e (i_q - \hat{i}_q) \tag{15}$$

where k_2 and τ_2 represent the PI coefficients of Ψ_f's adaptive law.

5.3 Design of Gain Matrix

For the system's linear forward path in Fig. 4, its transfer function matrix is

$$H(s) = [sI - (A + G)]^{-1} \tag{16}$$

The Kalman-Yacubovich-Popov Positive Real Lemma states that "$H(s)$ will be a severe positive real matrix, if the following equation is tenable

$$A + G + (A + G)^{\mathrm{T}} = -Q \tag{17}$$

where Q is a positive definite and real symmetric matrix, in a controllable and observable system Eq. (9)" [20].

After substitution of A and G into Eq. (17), we have

$$
\begin{cases}
\frac{R_s}{L_d} + g_{11} = \frac{R_s}{L_q} + g_{22} > 0 \\
\frac{L_d}{L_q} \omega_e + g_{12} = \frac{L_q}{L_d} \omega_e + g_{21}
\end{cases}
\tag{18}
$$

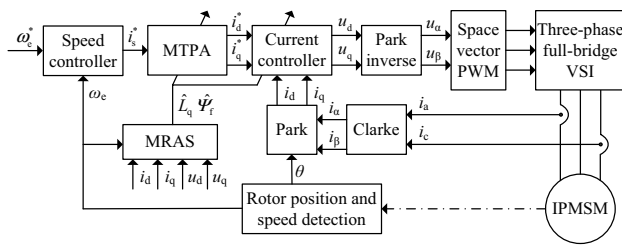**Fig. 5** Structure diagram of IPMSM MTPA control system

Table 1 Parameters of IPMSM

Rated power	20 kW
Rated torque	72 N m
Rated speed	3000 r/min
d-axis inductance	0.33 mH
q-axis inductance	0.63 mH
Rotor flux linkage	0.068 Wb

Table 2 Parameters of estimator

L_q's adaptive law—k_1	0.96
L_q's adaptive law—τ_1	0.001
Ψ_f's adaptive law—k_2	0.12
Ψ_f's adaptive law—τ_2	0.0088
Gain matrix–m	3
L_q's adaptive law—k_1	0.96

Based on the principle of the Popov Hyper Stability Theorem [20], the gain matrix G's elements should be configured as Eq. (18) restricts.

The characteristic equation of the adjustable model Eq. (9) is

$$\det(s\boldsymbol{I} - (\boldsymbol{A} + \boldsymbol{G})) = \begin{vmatrix} s + \frac{R_s}{L_d} + g_{11} & -\frac{L_q}{L_d}\omega_e + g_{12} \\ \frac{L_d}{L_q}\omega_e - g_{21} & s + \frac{R_s}{L_q} + g_{12} \end{vmatrix} = 0 \quad (19)$$

Considering the designed estimator's asymptotic stability and dynamic responses, the real parts of the closed-loop poles in the adjust model should be set m times as great as those in the reference model and be located at 135° and 225° in the complex plane ($m=2$–4), separately [21]. And then combining with the limitation of Eq. (18) yields

$$\begin{cases} 2\left(\frac{R_s}{L_d} + g_{11}\right) = m\left(\frac{R_s}{L_d} + \frac{R_s}{L_q}\right) \\ \left(\frac{R_s}{L_d} + g_{11}\right)^2 = \left(\frac{L_q}{L_d}\omega_e - g_{21}\right)^2 \end{cases} \quad (20)$$

Thus, from Eq. (18) and Eq. (20), the elements of the gain matrix G should be configured as follows

$$\boldsymbol{G} = \begin{bmatrix} -\left(\frac{m-2}{2}\frac{R_s}{L_d} + \frac{m}{2}\frac{R_s}{L_q}\right) & \frac{m}{2}\left(\frac{R_s}{L_d} + \frac{R_s}{L_q}\right) - \frac{L_q}{L_d}\omega_e \\ -\frac{m}{2}\left(\frac{R_s}{L_d} + \frac{R_s}{L_q}\right) + \frac{L_d}{L_q}\omega_e & -\left(\frac{m}{2}\frac{R_s}{L_d} + \frac{m-2}{2}\frac{R_s}{L_q}\right) \end{bmatrix} \quad (21)$$

To sum up, an overall structure of MTPA control system for an IPMSM is demonstrated in Fig. 5.

6 Simulation Results and Analysis

A simulation model of MTPA control system for an IPMSM system is established and tested in MATLAB. The prototype motor's parameters are listed in Table 1, where the average values within the speed/torque operation area are used for the inductances and the flux linkage. The estimator's key parameters are shown in Table 2.

In the simulation model, the space vector PWM inverter is considered to be an ideal amplifying element beneficial to prove the feasibility and validity of the used identification method avoiding disturbance from the inverter's nonlinearity. Besides, the DC bus voltage is 320 V, and hence the maximal amplitude of the inverter's output phase voltage can be calculated as follows

$$\frac{V_{DC}}{\sqrt{3}} = \frac{320V}{\sqrt{3}} \approx 185V \quad (22)$$

Figures 6, 7 and 8 display the estimation effect of parameter, changing to $90\%L_q$, $110\%\Psi_f$ and both of them, separately. When the parameters vary as mentioned above, the current errors e_d and e_q are convergent to zero quickly. Also, the estimated parameters approach rapidly the anticipant ones. In consequence, the proposed parameter estimator exhibits excellent tracking properties under the circumstance of parameter variance.

Comparisons of current tracking responses between the parameter invariance method and the parameter identification method are revealed in Figs. 9, 10 and 11. And L_q goes down by 10% in Fig. 9, Ψ_f goes up by 10% in Fig. 10, and both of them occur in Fig. 11.

Evidently, with the former method, the static dq-axis currents are so different from the expected ones that the resulting MTPA trajectory deflects greatly from the optimal one. Nevertheless, the latter method is able to force the current operating point into approaching the optimal MTPA trajectory immediately. Accordingly, the presented design method increases significantly the system's robustness against parameter perturbations for MTPA control.
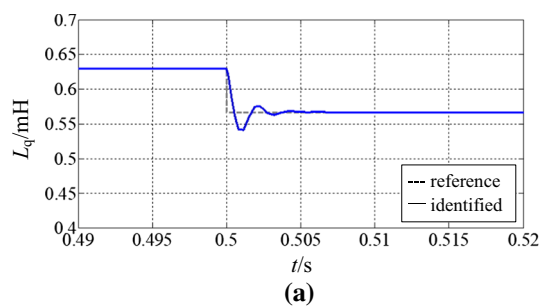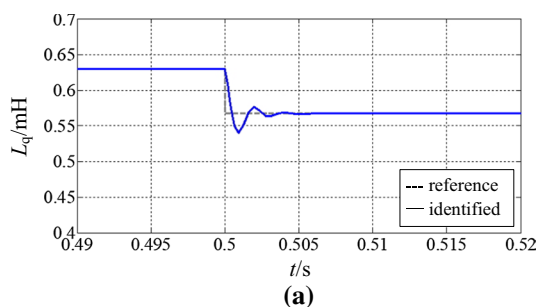
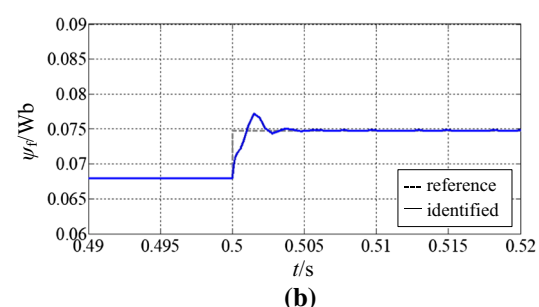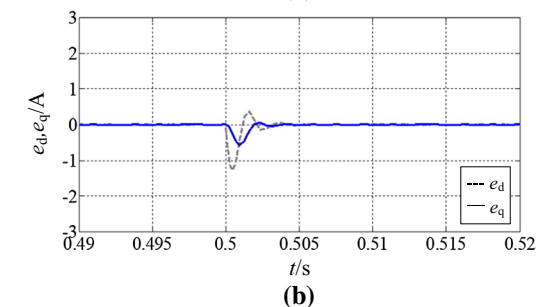**Fig. 6** Estimation effect of q-axis inductance
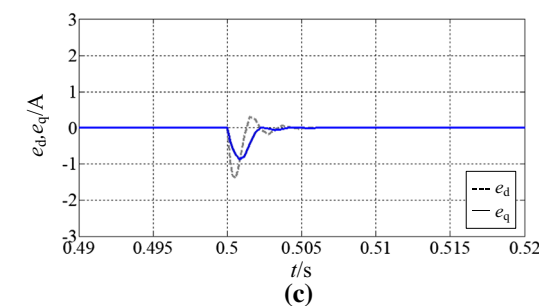

Fig. 7 Estimation effect of flux linkage

Fig. 8 Estimation effect of inductance and flux linkage
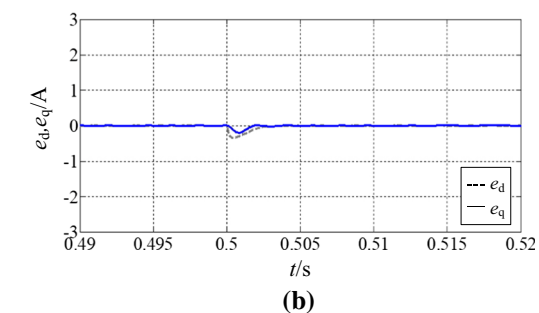
Fig. 9 Current responses with q-axis inductance variance

7 Experimental Results and Analysis

The experimental bench for the IPMSM drive and control system is exhibited in Fig. 12. In the experiment, the parameters of motor and estimator are identical with those in the simulation, as listed in Tables 1 and 2. And a three-phase full-bridge voltage source inverter are adopted with
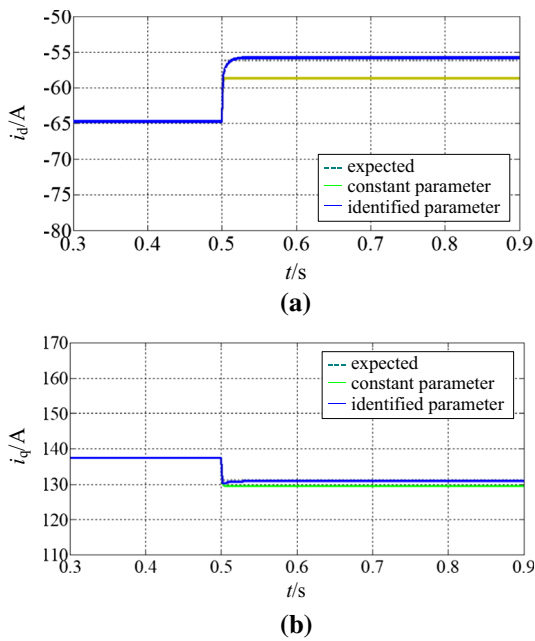
Fig. 10 Current responses with flux linkage variance
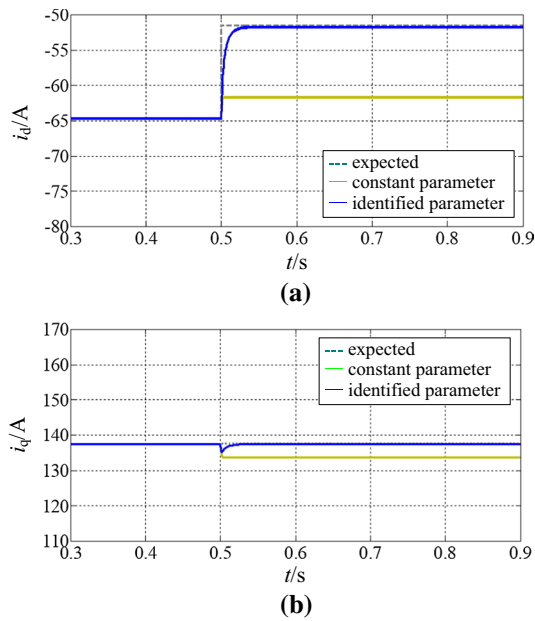
Fig. 11 Current responses with q-axis inductance and flux linkage variances

the space vector PWM method, where the DC bus voltage is 320 V, the switching frequency is 10 kHz and the dead time is 6.4 μs.

Figure 13 manifests the MTPA current operation points with the presented parameter identification method compared with the optimal torque-current characteristics. To calculate the dq-axis currents according to Eq. (3) and

Fig. 12 Experimental bench for IPMSM system
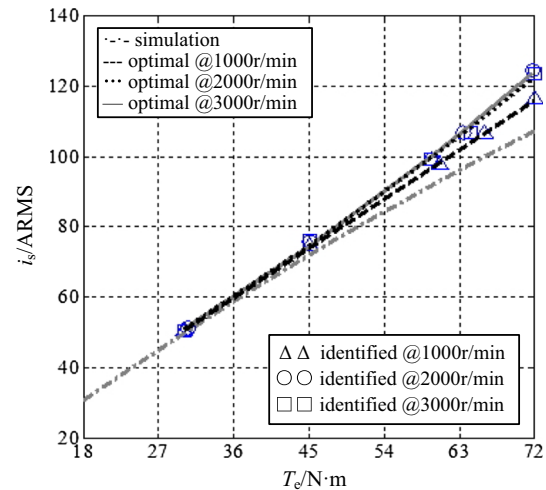
Fig. 13 Torque-current characteristics and MTPA operation points

Eq. (4) can plot a simulation waveform in Fig. 13, the parameter change not included. The optimal waveforms are gained by repeated modulation of torque angle β at each selected torque/speed operation point, where a torque point is chosen every 9 N m from light load (18 N m) to full load (72 N m). In the test, we recorded a group of the optimal data at each specified torque/speed point and stored the corresponding torque angle β in the look-up table (LUT). As stated above, the LUT method will cost a large amount of memory spaces and place a heavy burden on the off-line experiment. However, the resulting MTPA trajectories can be taken as the optimal torque-current characteristics, and thus be used to validate the performance and effect of the applied on-line parameter identification method. From Fig. 13, it is clear that the operation points with estimated parameters almost coincide with the optimal waveforms, so the designed MTPA control method has excellent static identification precision.

It can be found out that there are significant differences between the simulation waveforms and the measured

waveforms with on-line estimation, and the optimal waveform at 1000 r/min is also somewhat different from those at 2000 r/min and 3000 r/min, which diverges more greatly with the increase of torque. It is because the magnetic saturation has more remarkable influence on the motor's parameter perturbation and the MTPA working points at a higher torque or speed. For further explanation, the rotor flux linkage and the stator q-axis inductance are reduced by the saturated magnetic field, and then a larger current is required to generate a certain torque, as described in the torque expression Eq. (2). Additionally, the inverter's nonlinear output voltage will also lead to a difference between simulation and experiment, which can be improved by a dead-time compensation method [22].

Comparisons of load change responses between the LUT method and the identification method at the rated speed are shown in Figs. 14 and 15, where the torque is loaded from light load 18 N m to full load 72 N m suddenly at $t = 15.0$ s in Fig. 14, and the torque is unloaded from full load 72 N m to half load 36 N m abruptly at $t = 5.5$ s in Fig. 15. As explained above, the optimal torque angles in the off-line table are a set of reserved discontinuous data. And if the working condition (speed, torque, etc.) changes, the operation point may be reciprocating within a neighborhood of the target point, so the torque
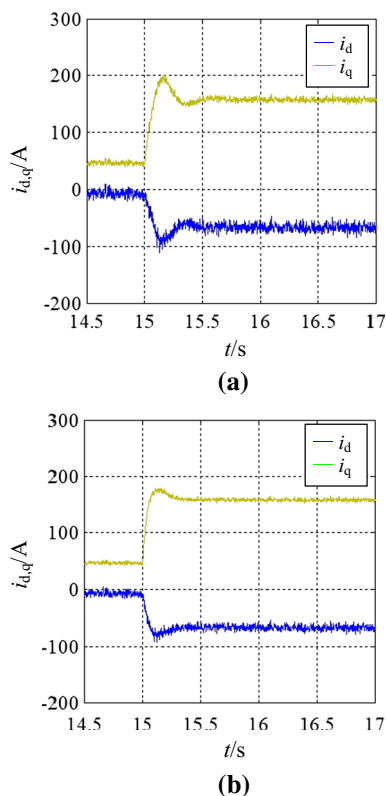

Fig. 14 Loading responses of currents with rated speed. **a** LUT. **b** Identification
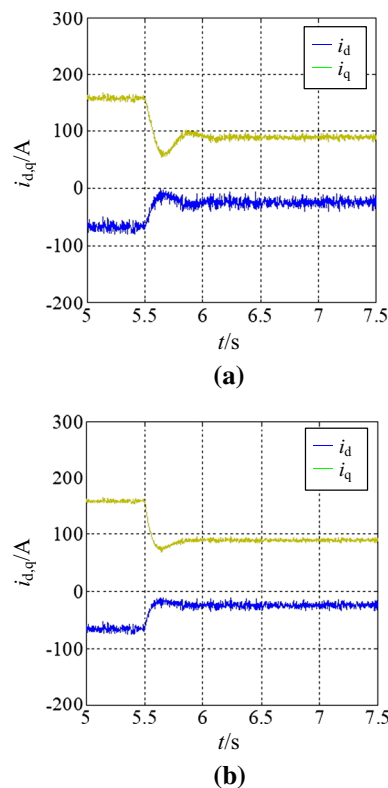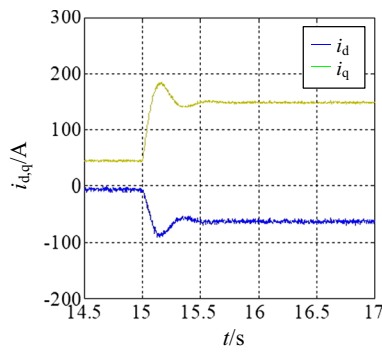

Fig. 15 Unloading responses of currents with rated speed. **a** LUT. **b** Identification

angle has to be switched frequently before the system arrives at a new balanced stability. Therefore, it must result in bad dynamic responses and even system oscillation. From Figs. 14 and 15, using the on-line identification based MTPA control method, the adjusting time becomes shorter, the overshoot decreases, and the static ripple is also weakened for the dq-axis current. Thus, the designed MTPA trajectory tracking control method owns better dynamic and static running qualities.

Figures 16 and 17 illustrate current responses of loading and unloading between the LUT method and the identification method at the speed 1000 r/min, where the torque change is identical with that at the rated speed.

It can be seen evidently that the static amplitudes of i_d and i_q at the two different speeds are almost the same with the load torque 18 N m and 36 N m. Whereas, this is not the case with the full load torque 72 N m, in details, the static currents' amplitudes are 62.7 Å and 149.5 Å at 1000 r/min, while they are 66.7A and 159.1A at 3000 r/min. To conclude, the stator currents at the two speeds are 114.7 Å and 122.0 Å, respectively, which complies with what is revealed and analyzed in Fig. 13.

Figures 18 and 19 are the system starting responses of the identification method compared with the LUT method. Obviously, during the starting process, the
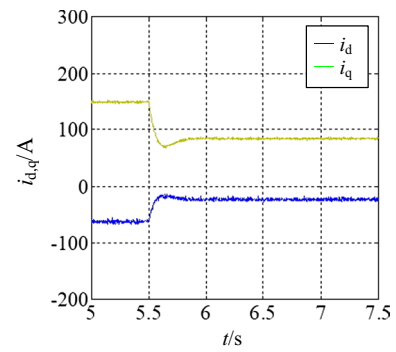
Fig. 16 Loading responses of currents with 1000 r/min. **a** LUT. **b** Identification
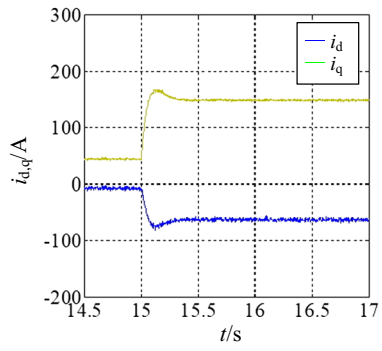
Fig. 17 Unloading responses of currents with 1000 r/min. **a** LUT. **b** Identification

speed's adjusting time is shorter, and its maximum overshoot is smaller with the identification method, so the designed MTPA control system can obtain good starting characteristics.

8 Conclusion

Aiming at a solution to the problems of MTPA trajectory deviation due to parameter change and rank-deficiency identification model, a full-rank estimator was designed with reference to the rotor flux linkage and the q-axis inductance, and the estimated parameters were used to update the stator current and accordingly track the MTPA trajectory on-line. The designed estimator is easy to realize and practical in engineering, and has excellent parameter identification effect. Simulation and experimental results verify that the proposed method improves greatly the static and dynamic performances of the MTPA control under the conditions of parameter perturbation and load disturbance, which can especially meet the high demand of torque's output capacity and dynamic response in application of EV motor drive. Furthermore, it needs further study and discussion on how the inverter nonlinearity will impact on the accuracy of parameter identification.
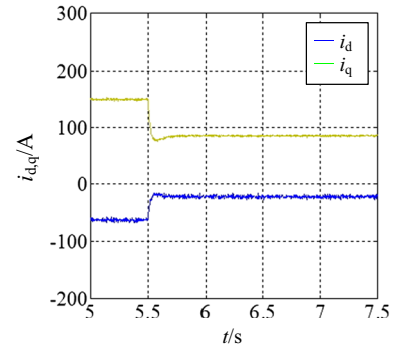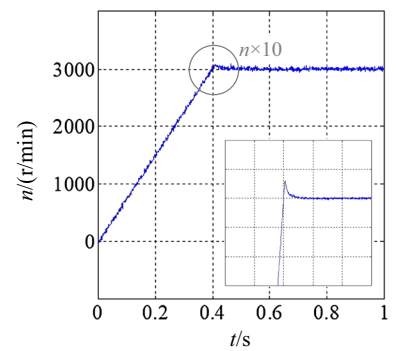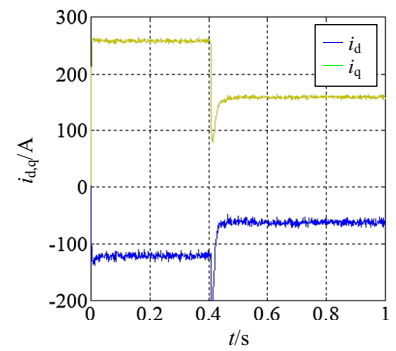

Fig. 18 System starting responses with LUT
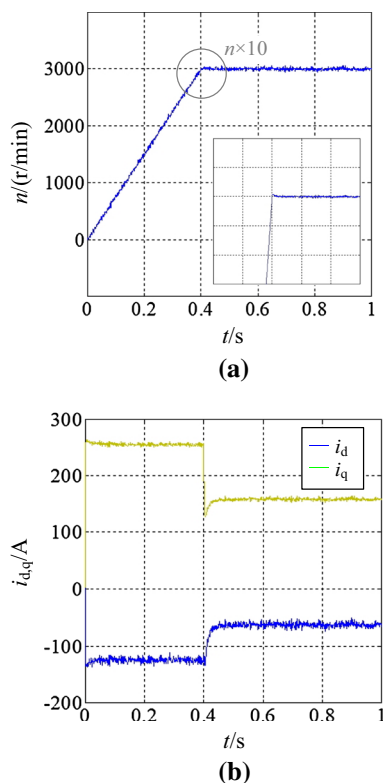
Fig. 19 System starting responses with identification

References

1. Jia C, Wang X, Liang Y, Zhou K (2019) Robust current controller for IPMSM drives Based on explicit model predictive control with online disturbance observer. IEEE Access 7:45898–45910

2. Ilka R, Alinejad-Beromi Y, Yaghobi H (2018) Techno-economic design optimisation of an interior permanent-magnet synchronous motor by the multi-objective approach. IET Electr Power Appl 12(7):972–978

3. Li K, Wang Y (2019) Maximum torque per ampere (MTPA) control for IPMSM drives based on a variable-equivalent-parameter MTPA control law. IEEE Trans Power Electron 34(7):7092–7102

4. Chowdhury MM, Haque ME, Saha S et al (2018) An enhanced control scheme for an IPM synchronous generator based wind turbine with MTPA trajectory and maximum power extraction. IEEE Trans Energy Convers 33(2):556–566

5. Jung SY, Hong J, Nam K (2013) Current minimizing torque control of the IPMSM using Ferrari's method. IEEE Trans Power Electron 28(12):5603–5617

6. Liu AH, Wang Y, Chen LC (2011) A self-checking method of MTPA for EV motors. China Patent 201010107606.7

7. Wang G, Li Z, Zhang G et al (2013) Quadrature PLL-based high-order sliding-mode observer for IPMSM sensorless control With online MTPA control strategy. IEEE Trans Energy Convers 28(1):214–224

8. Bedetti N, Calligaro S, Olsen C et al (2017) Automatic MTPA tracking in IPMSM drives: loop dynamics, design, and auto-tuning. IEEE Trans Ind Appl 53(5):4547–4558

9. Chen Q, Zhao W, Liu G et al (2019) Extension of virtual-Signal-injection-based MTPA control for five-phase IPMSM into fault-tolerant operation. IEEE Trans Industr Electron 66(2):944–955

10. Shi JF, Ge BJ, Lv YL et al (2018) Research of parameter identification of permanent magnet synchronous motor on line. Electr Mach Control 22(3):17–24

11. Liu J, Chen W (2016) Online multi-parameter identification for surface-mounted permanent magnet synchronous motors under quasi-steady-state. Trans China Electrotech Soc 31(7):154–160

12. Underwood SJ, Husain I (2010) Online parameter estimation and adaptive control of permanent magnet synchronous machines. IEEE Trans Indus Electr 57(7):2435–2443

13. Boileau T, Leboeuf N, Nahid-Mobarakeh N et al (2011) Online identification of PMSM parameters: parameter identifiability and estimator comparative study. IEEE Trans Ind Appl 47(4):1944–1957

14. Liu K, Zhang Q, Zhu ZQ et al (2010) Comparison of two novel MRAS based strategies for identifying parameters in permanent magnet synchronous motors. Int J Autom Comput 7(4):516–524

15. An QT, Sun L, Zhao K (2008) An adaptive on-line identification method for the parameters of permanent magnet synchronous motor. Trans China Electrotech Soc 23(6):31–35

16. Yang ZJ, Wang LN (2014) Online multi-parameter identification for surface-mounted permanent magnet synchronous motors. Trans China Electrotech Soc 23(9):111–118

17. Zhang YJ, Wang W, Zhang XQ et al (2017) Study on improved sliding-mode control with resistance estimation of PMSM. Electr Mach Control 21(6):10–17

18. Liu K, Zhang J (2010) Adaline neural network based online parameter estimation for surface-mounted permanent magnet synchronous machines. Proc IEEE 30(30):68–73

19. Shi T, Liu H, Chen W et al (2017) Parameter identification of surface permanent magnet synchronous machines considering voltage-source inverter nonlinearity. Trans China Electrotech Soc 32(7):77–83

20. Han ZZ, Chen PN, Chen SZ (2011) A textbook for adaptive control, vol 2. Tsinghua University Press, Beijing

21. Zhu Y, Wu S, Wu Z et al (2014) Precise torque control method of IPMSM in vehicle. Trans Chin Soc Agric Mach 45(1):8–13

22. Shen Z, Jiang D (2019) Dead-time effect compensation method based on current ripple prediction for voltage-source inverters. IEEE Trans Power Electron 34(1):971–983

Ningzhi Jin received the Ph.D. degree in electrical engineering from the Harbin University of Science and Technology (HUST), China, in 2012. He is currently an associate professor at the HUST. His research interests include power electronics, motor drive and control, and advanced nonlinear algorithms.

Guangyi Li is studying for a master's degree at the Harbin University of science and technology, China. His research interests are parameter identification and nonlinear algorithms in motion control.

Kai Zhou received the Ph.D. degree in electrical engineering from the Harbin University of Science and Technology, China, in 2012, where he was appointed as a professor in 2019. His research interests include automotive electronics, motor control and test technology, and new energy vehicles.

Jinfeng Liu received the Ph.D. degree in electrical engineering from the Harbin University of Science and Technology (HUST), China, in 2011. She is an associate professor at the HUST. Her research interests are motor control, distribution system and resonance compensation.

Herbert Ho-Ching Iu received the Ph.D. degree from the Hong Kong Polytechnic University in 2000. He is currently a professor at the University of Western Australia. His research interests include power electronics, renewable energy, nonlinear dynamics and memristor.